Available online at www.sciencedirect.com
ScienceDirect
Polymer 48 (2007) 3732–3738
polymer
www.elsevier.com/locate/polymer

A new approach in the study of tethered diblock copolymer surface morphology and its tethering density dependence

Huiming Xiong [a,1], Joseph X. Zheng [a], Ryan M. Van Horn [a], Kwang-Un Jeong [a], Roderic P. Quirk [a], Bernard Lotz [b], Edwin L. Thomas [c], William J. Brittain [a], Stephen Z.D. Cheng [a,*]

[a] *Maurice Morton Institute and Department of Polymer Science, University of Akron, Akron, OH 44325-3909, USA*
[b] *Institut Charles Sadron, Strasbourg 67083, France*
[c] *Department of Materials Science and Engineering, Massachusetts Institute of Technology, Cambridge, MA 02139, USA*

Received 30 March 2007; received in revised form 16 April 2007; accepted 21 April 2007
Available online 3 May 2007

Abstract

A poly(L-lactic acid)-*block*-polystyrene-*block*-poly(methyl methacrylate) (PLLA-*b*-PS-*b*-PMMA) triblock copolymer was synthesized with a crystalline PLLA end block. Single crystals of this triblock copolymer grown in dilute solution could generate uniformly tethered diblock copolymer brushes, PS-*b*-PMMA, on the PLLA single crystal substrate. The diblock copolymer brushes exhibited responsive, characteristic surface structures after solvent treatment depending upon the quality of the solvent in relation to each block. The chemical compositions of these surface structures were detected *via* the surface enhanced Raman scattering technique. Using atomic force microscopy, the physical morphologies of these surface structures were identified as micelles in cyclohexane and ''onion''-like morphologies in 2-methoxyethanol, especially when the PS-*b*-PMMA tethered chains were at low tethering density.

Keywords: Block copolymer; Single crystal; Surface morphology and chemical composition

1. Introduction

Over the past two decades, tethered polymer systems have attracted attention due not only to their theoretical interests but also their potential applicability [1–9]. Specific forms of particular interest are the ''mixed brushes,'' or ''binary brushes'' [10,11]. In these systems, two different homopolymer brushes are tethered to the same surface. The second form of interest is brushes composed of copolymers, either random [12] or block, with various architectures, such as diblock copolymers [13,14], Y-shaped block copolymers [15,16], and others. Theoretical studies have predicted interesting surface morphologies for these systems, for example, ''ripple,'' ''dimple,'' ''onion,'' ''garlic,'' and ''stripe'' morphologies [17–20]; however, long-rang order and periodicity are seldom observed experimentally due to composition fluctuations and broad tethering point distributions [21]. There are still great challenges for the conventional methods of chemical ''grafting to'' and ''grafting from'' and physical adsorption. For example, the major disadvantage of chemically ''grafting to'' and physical adsorption methods is that their average grafting densities are usually low due to the molecular shielding effect near the substrate; while the disadvantages of the ''grafting from'' method are the less controlled molecular weight and molecular weight distribution as well as the non-uniform tethering density. In this article, we present a novel approach with which the tethering density can be accurately tuned with a uniform distribution. We believe that this approach provides a new way to examine the theoretical predictions of surface morphologies.

The experimental method presented here dates back to the 1960s [22]. Lotz and Kovacs found that crystalline–amorphous poly(ethylene oxide)-*block*-polystyrene (PEO-*b*-PS)

* Corresponding author.
E-mail address: scheng@uakron.edu (S.Z.D. Cheng).
[1] Present address: Center for Functional Nanomaterials, Brookhaven National Laboratory, Upton, NY 11973, USA.

0032-3861/$ - see front matter © 2007 Elsevier Ltd. All rights reserved.
doi:10.1016/j.polymer.2007.04.067

copolymers can grow single crystals in dilute solution. In this system, the PS blocks can be viewed as being tethered on the basal surfaces of the PEO block single crystal (substrate). Recently, we have utilized this method of growing lamellar single crystals to probe the physics of each of the polymer brush regimes by controlling molecular weights and crystallization temperature (T_x) of a PEO or poly(L-lactic acid) (PLLA) block. Through the precise control of these parameters, the thickness of the single crystal and thus, the number of folds, are fixed. This leads to a tunable tethering density [23,24]. In other words, the tethering density can be adjusted by changing T_x, or undercooling (ΔT), and/or the molecular weights of the PEO or PLLA crystalline blocks.

We now use triblock copolymers such as poly(L-lactic acid)-*block*-polystyrene-*block*-poly(methyl methacrylate) (PLLA-*b*-PS-*b*-PMMA), of which the crystallizable block is located at one end of the triblock copolymer, to generate uniformly tethered diblock copolymer (PS-*b*-PMMA) chains. By growing lamellar single crystals of PLLA blocks in dilute solution, we generate tethered diblock copolymer chains on both sides of the PLLA crystalline substrate. We are interested in the changes of the physical surface patterns as well as their chemical compositions at the surface at different tethering densities. Namely, what will be observed for the tethered diblock copolymers after they are treated in different types of solvent?

2. Experimental section

A PLLA-*b*-PS-*b*-PMMA triblock copolymer was prepared. A triblock copolymer, poly(L-lactic acid)-*block*-polystyrene-*block*-poly(methyl methacrylate) (PLLA-*b*-PS-*b*-PMMA), was prepared by first synthesizing hydroxyl-functionalized PS-*b*-PMMA as a macroinitiator and followed by a coordination–insertion polymerization of L-lactide using the PS-*b*-PMMA as the initiator and triethylaluminum as a catalyst. This macroinitiator was synthesized *via* a sequential anionic polymerization of styrene and methyl methacrylate using a protected hydroxyl-functionalized initiator.

For molecular analyses, ^{1}H nuclear magnetic resonance (NMR) was used. ^{1}H NMR spectra were recorded in $CDCl_3$ (99.8% D, Cambridge Isotope Laboratories) on Varian Mercury 400 MHz spectrometer at room temperature. The NMR sample concentration was usually chosen to be 10–20 wt% in deuterated solvent. For the sample containing alkylsilyl groups, trimethylsilane (TMS) was not used as an internal standard. Size exclusion chromatography (SEC) experiments were conducted using the Waters 150-C Plus instrument equipped with a differential refractometer, a viscosity detector (Viscotek Model 150R) and four Phenomenex Phenogel columns (50, 10^2, 10^3 and 10^4 nm). The SEC measurement was carried out in tetrahydrofuran (THF) at 30 °C at a flow rate of 0.5 mL/min with calibration by polystyrene standards.

Since the PLLA blocks are crystalline, we can utilize the well-established self-seeding technique [22,25] to grow single crystals of the triblock copolymers. Typically, the copolymer sample solution was made with amyl acetate at a concentration of 0.005 (wt) % or less. The solution was then heated above the dissolution temperature (130 °C) in an oil bath and kept there for 10 min. The homogeneous solution was then quenched to room temperature and left overnight to allow the crystallization of the PLLA block. Subsequently, the sample was heated to a seeding temperature ($T_s = 110$ °C) and held there for 10 min to dissolve most of the crystals (over 99 %) but leaving a small amount of crystal nuclei (as seeds). The solution was then quickly transferred to another isothermal oil bath with a preset T_x, *e.g.*, 85 °C. Isothermal crystallization times of about 1 day were required to complete the single crystal growth. The exact crystallization time is dependent on T_x or undercooling (ΔT).

After the growth was finished, the single crystals were dried by a stream of nitrogen. Single crystal morphology was first observed in a transmission electron microscope (TEM, FEI Tacnai 12) with an accelerating voltage of 120 kV. To achieve a higher contrast in the TEM micrograph, the samples were sometimes shadowed by Pt at a tilting angle of 25°. Selected area electron diffraction (SAED) experiments were also conducted to determine the chain orientation in the copolymer single crystals. Calibration of the SAED spacing values smaller than 0.384 nm was carried out using evaporated thallous chloride, which has the largest first-order spacing diffraction of 0.384 nm. Spacing values larger than 0.384 nm were calibrated by doubling the *d*-spacing values of the first-order diffractions.

In order to measure the overall single crystal thickness and identify the surface morphologies *via* surface stiffness changes on the single crystals, the crystals grown were also dried and prepared for observations under an atomic force microscope (AFM, Nanoscope IIIA). The height and phase images provide insight into the surface topologies of the tethered PS-*b*-PMMA diblock copolymers on the PLLA lamellar substrate. A silicon tip in the tapping mode was utilized. During AFM scanning, the cantilever tip-to-sample force needed to be carefully adjusted to avoid artifacts. For the tip-to-sample force, a large force could lead to tip penetrations into the thin tethered chain layers, and disturb the materials at the layer surfaces. Therefore, we carefully adjusted the value of r_{sp}, which is the ratio of the set-point amplitude to the driving amplitude, to make sure that the tip did not damage the surface topologies, yet the surface profiles could still be monitored. All the AFM raw data were carefully analyzed using the first-order planefit procedure. A scan rate of 1 Hz and a resolution of 512 × 512 were selected to generate high quality images.

Surface enhanced Raman scattering (SERS) was conducted on a Bruker model RFS 100 Fourier Raman spectrometer. The incident laser excitation was 1064 nm from an Nd:YAG laser source. The output was 100 mW. The Raman scattering was measured at an angle of 180°. The silver mirror was prepared by dipping a clean glass plate into a solution of silver ammonia complex and formaldehyde. The silver ions were reduced to form silver particles deposited on the glass plate. The glass plate was washed with distilled water and ethanol several times and then, dried under high vacuum overnight. The single crystal solutions, either in cyclohexane or 2-methoxyethanol at 60 °C, were dropped onto the glass plates and quickly dried by

a stream of nitrogen. The glass plates were then dried under high vacuum overnight and were ready for further measurements. In order to identify the FT-SERS spectra of tethered diblock copolymers, we also carried out the SERS experiments on PS and PMMA homopolymers after the same solvent treatment procedures.

3. Results and discussion

3.1. Synthesis of hydroxyl-functionalized PS-b-PMMA and PLLA-b-PS-b-PMMA triblock copolymers

A protected functionalized initiator [the isoprene chain extended analog of 3-(trimethylsiloxyl)-1-propyllithium (NPFI-1100CE2)] was used to initiate the polymerization of styrene. Lithium chloride (0.19 g, 4.5 mmol) was added to the reactor and was dried at 150 °C overnight under dynamic vacuum. After cooling the reactor, NPFI-1100CE2 (0.61 mL, 1.5 M) was injected into the reactor under an argon atmosphere. After the reactor was evacuated, benzene (100 mL) was distilled into the reactor under vacuum using a dry ice/isopropyl alcohol bath. The reactor was then flame-sealed from the vacuum line. THF (5 mL, 5 vol%) was added by smashing the breakseal of the THF ampoule followed by addition of styrene (10 mL, 87.4 mmol). The orange-red color developed soon after the addition of styrene. This indicates the onset of polymerization. The solution was stirred overnight, and a portion of the poly(styryl)lithium solution was removed into an ampoule and sealed off as a base polystyrene sample. The reactor was reconnected to the vacuum line, and benzene was removed by distillation on the vacuum line. THF (100 mL) was distilled into the reactor at −78 °C using a dry ice/isopropyl alcohol bath. The reactor was again flame-sealed from the vacuum line. The poly(styryl)lithium solution was then reacted with 1,1-diphenylethylene (0.32 mL, 1.8 mmol) by breaking the breakseal of the ampoule. The solution was allowed to react for 2 h at −78 °C. The color of the solution turned to dark red soon after addition of 1,1-diphenylethylene. The methyl methacrylate (9.7 mL, 97 mmol) was then added slowly to the solution over 1 h. The dark red color gradually changed to green. The temperature of the reactor was kept at −78 °C using the dry ice/isopropyl alcohol bath. The reaction was conducted for 2 h and terminated by methanol. The product was precipitated into methanol, collected and dried on the vacuum line for 24 h.

The PS-*b*-PMMA diblock copolymer with a protected hydroxyl group (10 g, 540 mmol) was dissolved in THF. Drops of hydrochloric acid were added to the solution using a pipette, and it was stirred overnight at room temperature to remove the protecting group. The product was precipitated into methanol, collected and dried on the vacuum line for 24 h. The completion of the deprotection reaction was checked by ^{1}H NMR as shown in Fig. 1.

An α-hydroxylated diblock copolymer PS-*b*-PMMA (1 g, 0.054 mmol, $M_n = 18.5$ kg/mol, $M_w/M_n = 1.03$) was dissolved in 8 mL of purified toluene and reacted with triethylaluminum

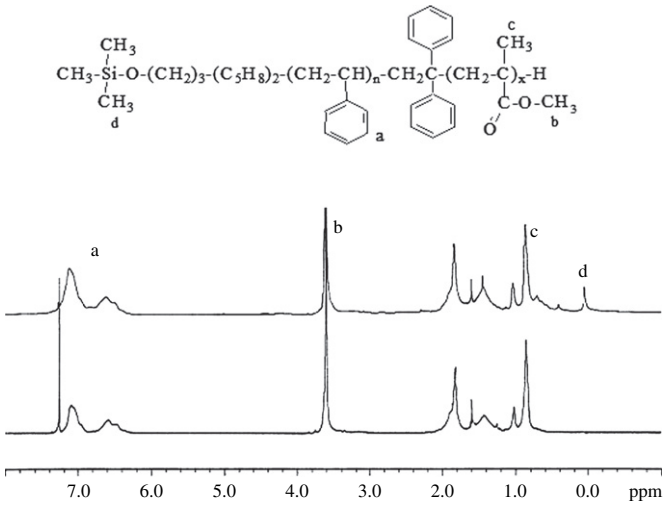

Fig. 1. ^{1}H NMR ($CDCl_3$) of PS-*b*-PMMA diblock copolymer ($M_n = 18.5 \times 10^3$ g/mol) before (top) and after (bottom) deprotection.

(0.06 mL, 0.06 mmol, 1 M, Aldrich) in the dry box. The reaction solution was stirred overnight and L-lactide (1 g, 6.9 mmol) was added to the solution in the dry box. The flask was taken out of the dry box and heated at 60 °C using an oil bath for 5 days. The reaction was terminated by acidic methanol (0.1 % HCl) and precipitated into methanol. The purified sample was collected and dried in a vacuum oven at room temperature for one day. The triblock copolymer chemical structure and molecular weights are shown in Figs. 2 and 3 based on ^{1}H NMR and gel permeation chromatographic results, respectively. The final molecular weights of the triblock copolymer are 21.6 kg/mol (PLLA), 7.5 kg/mol (PS), and 11 kg/mol (PMMA), respectively, with a polydispersity of 1.07.

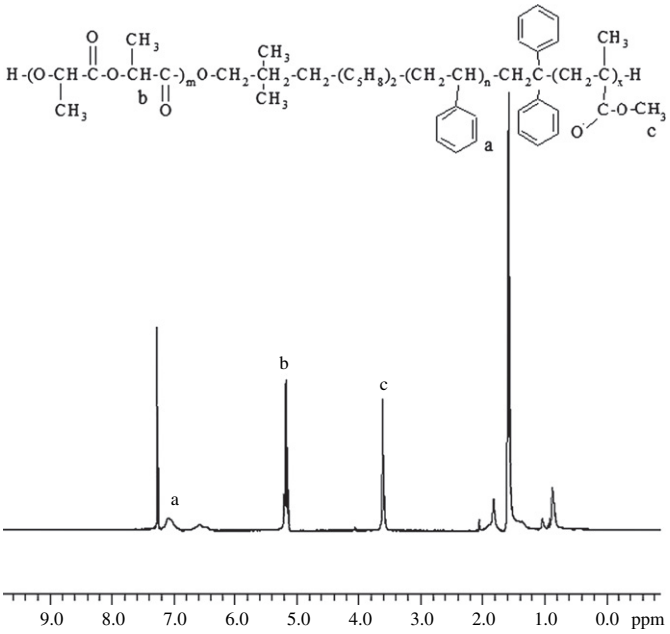

Fig. 2. ^{1}H NMR ($CDCl_3$) of PLLA-*b*-PS-*b*-PMMA triblock copolymer (21.6×10^3 g/mol−7.5×10^3 g/mol−11.0×10^3 g/mol).

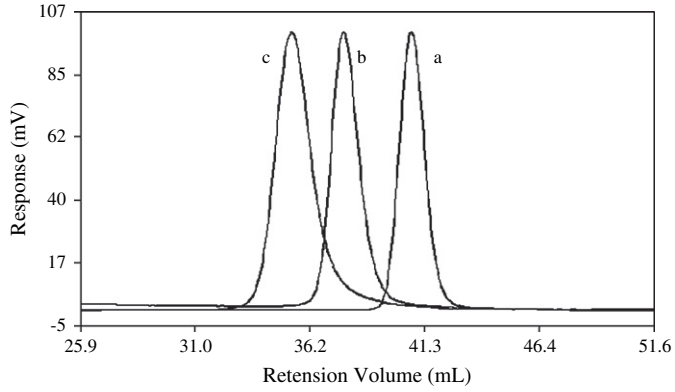

Fig. 3. SEC chromatograms of the base polystyrene ($M_{n(SEC)} = 7.5 \times 10^3$ g/mol) (a), the hydroxylated PS–PMMA (11.0×10^3 g/mol–7.5×10^3 g/mol) (b) and PLLA-*b*-PS-*b*-PMMA (21.6×10^3 g/mol–7.5×10^3 g/mol–11.0×10^3 g/mol) (c).

3.2. Single crystal growth, surface chemical composition and morphology changes

Fig. 4 shows lozenge-shaped PLLA single crystals observed in AFM (left, height image) and TEM (right, bright image). This type of single crystal can grow to a lateral size up to several hundred micrometers. An SAED pattern is also included in this figure as an inset. Based on this ED pattern, four (110) and two (200) diffractions can be identified, indicating that this is a [001] zone ED pattern of an orthorhombic lattice of the α-modification of PLLA crystals [26–29]. The single crystals are thus bounded by four (110) crystalline planes, and the PLLA chain direction is parallel to the single crystal surface normal.

By immersing the single crystals in cyclohexane (good solvent for PS) or 2-methoxyethanol (good solvent for PMMA) at 60 °C and an immersion time of 30 min, we have found that the tethered diblock copolymer (PS-*b*-PMMA) chemical composition at the surface and physical morphology are switched. First, for the determination of the chemical composition change, we chose to utilize the SERS technique that is sensitive to surface chemical composition at a depth of about 1 nm [30–32]. The top spectrum of Fig. 5a is obtained after

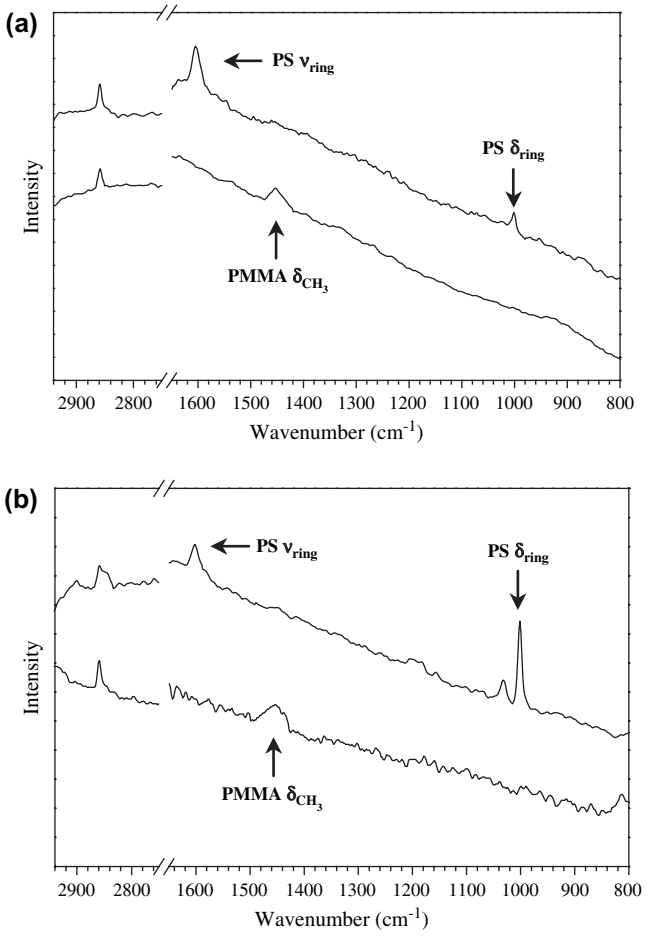

Fig. 5. SERS spectra of PLLA-*b*-PS-*b*-PMMA single crystals after immersion in cyclohexane (top) and 2-methoxyethanol (bottom) at 60 °C for 30 min (a); SERS spectra of homopolymer PS (top) and PMMA (bottom) after treatment in the same conditions as in (a) (b).

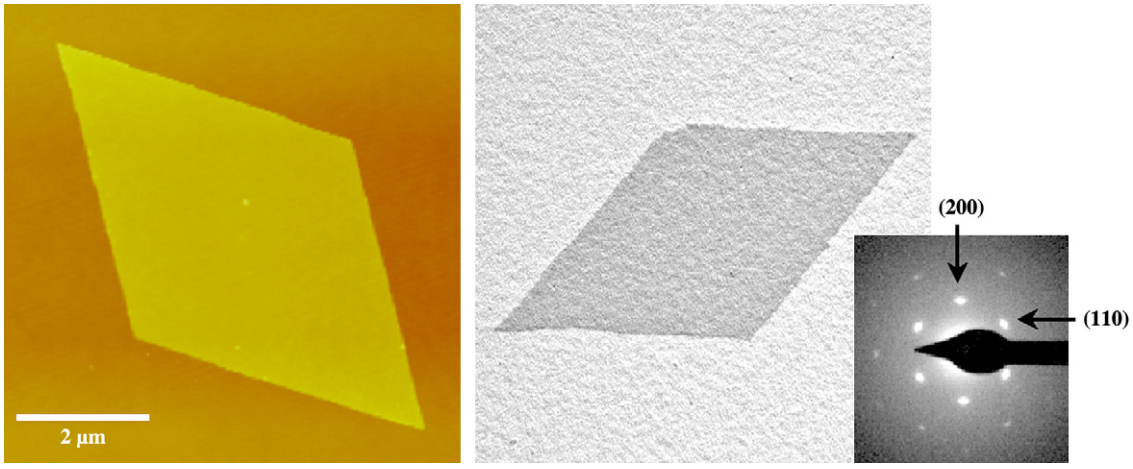

Fig. 4. AFM height image (left) TEM bright image (right) of a PLLA-*b*-PS-*b*-PMMA lamellar single crystal grown in amyl acetate at 75 °C. The inset is the [001] zone ED pattern of the single crystal in TEM (the electron diffraction pattern is not in the orientation with the single crystal morphology). The maximum *Z*-scale of AFM height image is 30 nm.

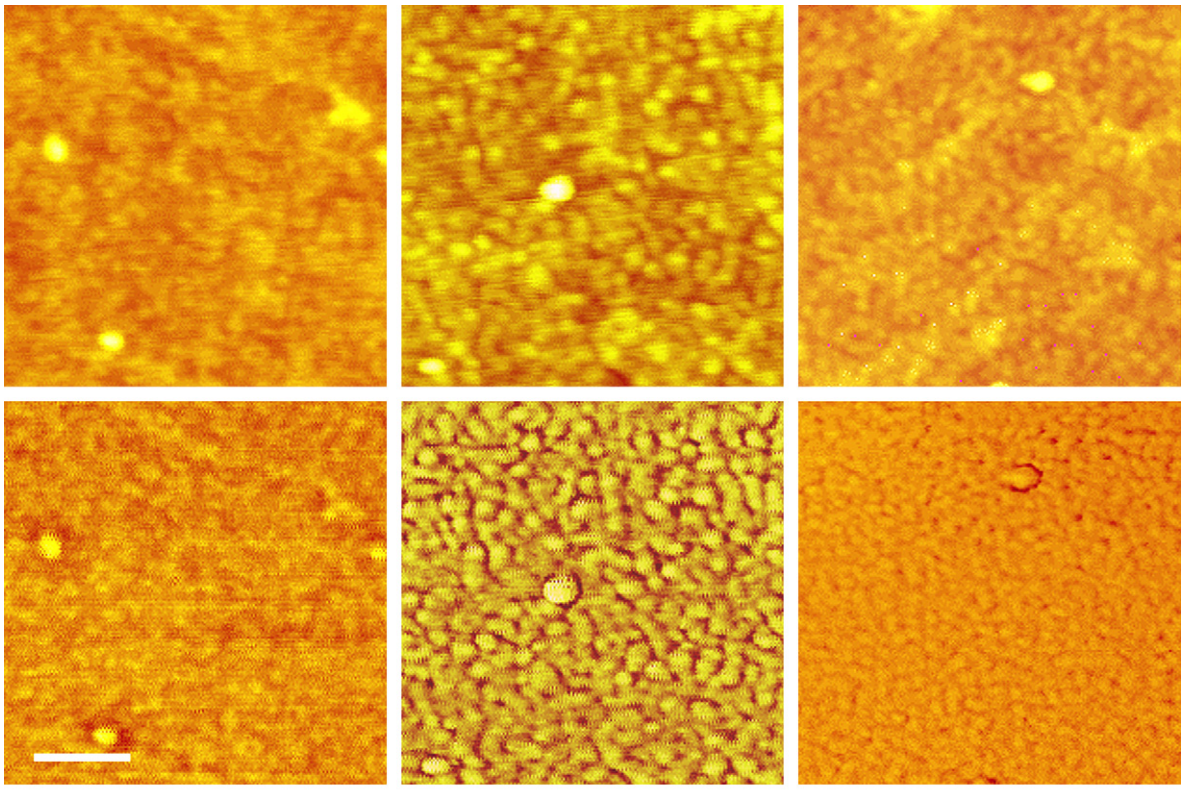

Fig. 6. AFM images of the PLLA-*b*-PS-*b*-PMMA triblock copolymer single crystal surface after treatment with cyclohexane when the crystal was grown in *p*-xylene at $T_x = 60\,^{\circ}C$ with the lowest tethering density (a), the crystals were grown in amyl acetate at $T_x = 75\,^{\circ}C$ (b) and 85 °C (c). The figures in the top are height images, the maximum *Z*-scale is 5 nm. The figures on the bottom are phase images, the maximum *Z*-scale is 5°. The scalar bar is 100 nm.

treatment with cyclohexane, a good solvent for PS. It shows two characteristic vibrations associated with PS, one at 1605 cm^{-1} (C–C in-plane stretching of the benzene rings) and one at 1000 cm^{-1} (“breathing” mode of benzene rings). These results indicate that the PS middle blocks were brought to the surface and contacted the silver mirror substrate for enhanced signal response. It can be assumed that the PMMA end blocks form collapsed cores in this case and are surrounded by the PS blocks. After the single crystals were treated with 2-methoxyethanol, the vibrations associated with PS are no longer observed, only the characteristic vibration of PMMA at 1453 cm^{-1} ($-CH_3$ symmetric deformation) can be seen (the bottom spectrum of Fig. 4a). The PMMA blocks now stay at the surface, and the PS blocks form the collapsed cores. The peaks at 2850 cm^{-1} are attributed to $-CH_2-$ stretching, which exists in both PS and PMMA blocks. The identification of the PS and PMMA blocks at the surfaces can be further verified by comparing the spectra in Fig. 5a with the SERS spectra of homopolymer PS and PMMA after immersion in the same solvents (see Fig. 5b).

The physical morphologies of the PS-*b*-PMMA tethered chains on single crystal substrates were studied using AFM in tapping mode. The single crystals of the PLLA-*b*-PS-*b*-PMMA triblock copolymer were grown at different T_x's, 85 °C and 75 °C in amyl acetate and 60 °C in *p*-xylene. The thicknesses determined by the AFM height images are about 14, 12, and 10 nm, respectively. After calculation of the volume fraction of the crystalline blocks, we can estimate the thickness of the single crystal part (PLLA) to be 7.1, 6.1, and 5.1 nm, respectively [23,24]. Based on the molecular weight and crystal unit cell of the α-modification of PLLA (orthorhombic, $a = 1.06$ nm, $b = 0.61$ nm, $c = 2.88$ nm) [28], we can obtain the tethering densities of the system. They are 0.13 nm^{-2} at 85 °C, 0.11 nm^{-2} at 75 °C, and 0.091 nm^{-2} at 60 °C, respectively.

The surface morphologies are found to be responsive to different solvent treatments. As shown in Fig. 6a of which the single crystal was grown in *p*-xylene at $T_x = 60\,^{\circ}C$ with the lowest tethering density, after the sample was treated with cyclohexane, the surfaces appear to contain nodules. The nodular morphologies are thought to be micelles with the PMMA end blocks collapsed to form cores, supported and covered by the PS middle blocks. Since the glassy PS and PMMA at room temperature exhibit different hardnesses, AFM can thus be used to distinguish the difference between them. Macroscopically, PMMA is harder than PS based on the Rockwell hardness. For PMMA, the Rockwell hardnesses is M80–M105, while for PS, it is M65–M85 [33]. Microscopically, the depth of a static indentation for an AFM tip penetrating into PS domains is approximately 5 nm, while a tip penetrating into PMMA domains is less than 1 nm [34]. The PMMA nodules in the phase image should be attributed to the fact that the AFM tip was penetrating into the PS matrix. This does not indicate that the PMMA nodules

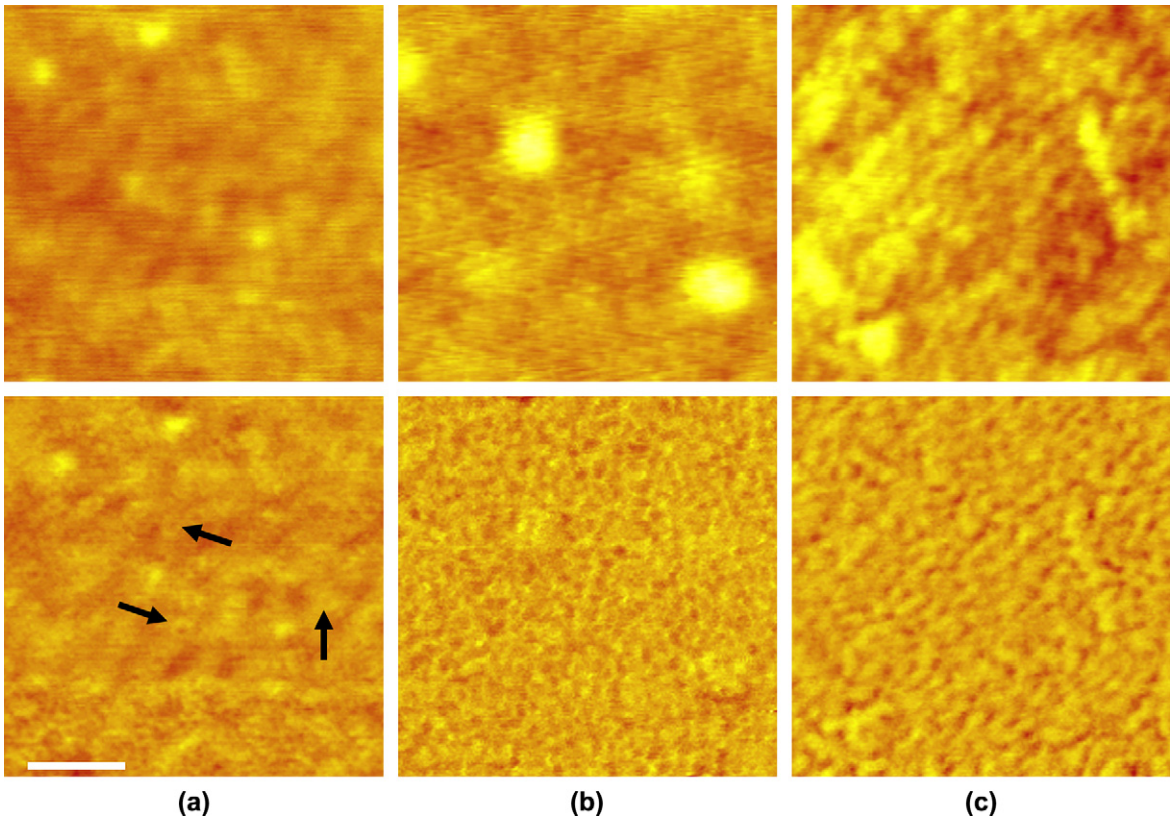

Fig. 7. AFM images of the PLLA-*b*-PS-*b*-PMMA triblock copolymer single crystal surface after treatment with 2-methoxyethanol when the crystal was grown in *p*-xylene at $T_x = 60\,^{\circ}C$ with the lowest tethering density (a), the crystals were grown in amyl acetate at $T_x = 75\,^{\circ}C$ (b) and 85 °C (c). The figures in the top line are height images, the maximum *Z*-scale is 5 nm. The figures on the bottom are phase images, the maximum *Z*-scale is 5°. The scalar bar is 100 nm.

are on the surface. In fact, the SERS results have shown that the PS blocks are the only chemical composition on the surface. The characteristic size is much smaller than those generated by the chemically ''grafting from'' method [13,14]. As the tethering density increases, the micelles stay closer. This can be seen in Fig. 6b and 6c. Note that these two figures show the surface morphologies as the tethering density increases (the single crystals were grown at $T_x = 75\,^{\circ}C$ and 85 °C in amyl acetate).

On the other hand, after treatment with 2-methoxyethanol, the middle PS blocks collapse to form the cores, and the PMMA blocks surround them to be the shells. In particular, when the crystal was grown in *p*-xylene at $T_x = 60\,^{\circ}C$ with the lowest tethering density, the morphologies become more blurred and rather broad as seen in the height image of Fig. 7a. The phase image in Fig. 7a shows more or less regular ''onion''-like morphologies with softer (dark) PS cores surrounded by harder (bright) PMMA shells at a low tethering density (see arrows in Fig. 7a). We believe that in the characteristic size of the surface structures in our system the AFM tip can reach both the soft PS cores and the hard PMMA shells of the onion structure. As theoretically predicted [17–20], the surface morphologies are more pronounced at sparse tethering densities, and when the tethering density increases, the neighboring PMMA shells start to overlap. This overlap gives rise to continuous domains as revealed by the phase images of tethered PS-*b*-PMMA diblock copolymer at higher tethering densities as shown in Fig. 7b and 7c. A schematic drawing of these nodular and ''onion''-like morphologies at a low tethering density is shown in Fig. 8.

Reasons for this observation could be that in our approach the tethered polymer chain system is well-defined and the tethered diblock copolymer possesses uniform chemical compositions and tethering density. Note that since the tethered diblock copolymers are on both sides of the PLLA block single crystal, the tethering density calculation needs to take this factor into account. Since the tethering density of this diblock copolymer is 0.091 nm^{-2} and the average area occupied by one ''onion'' is ~400 nm^2 (the number of ''onions'' per unit area in Fig. 7a), the number of the tethered PS-*b*-PMMA chains in one ''onion'' can be estimated to be ~36 chains.

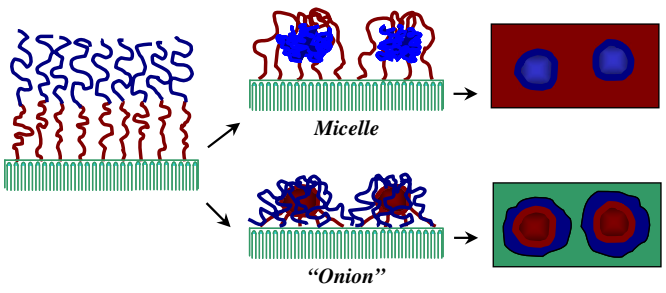

Fig. 8. Schematic drawing of these nodular and ''onion''-like morphologies at a low tethering density.

4. Conclusion

In summary, we have synthesized a triblock copolymer PLLA-*b*-PS-*b*-PMMA and generated uniformly tethered PS-*b*-PMMA diblock copolymers by growing lamellar single crystals of a triblock copolymer with a PLLA crystalline end block. The tethered copolymers respond to the selective solvent treatment to form characteristic surface morphologies. At a sparse tethering density, the ''onion''-like morphology has been observed after treatment with 2-methoxyethanol. We are also selecting other possible neutral solvents for this system to further extend our study on the surface morphologies of the PS-*b*-PMMA diblock copolymer. This approach is potentially applicable to other tethered polymer systems, such as Y-shaped polymer brushes using 3-arm block copolymers with one crystalline block. Work is currently being done with these systems. We hope these resulting model systems can provide a robust approach to verify the predictions of theoretical work and offer guidance for further active research on tethered polymer systems.

Acknowledgment

This work was supported by NSF (DMR-0516602).

References

[1] Zhao B, Brittain WJ. Prog Polym Sci 2000;25:677–710, the references cited therein.
[2] Kent MS. Macromol Rapid Commun 2000;21:243.
[3] Rühe J, Knoll W. J Macromol Sci Polym Rev 2002;C42:91.
[4] Satulovsky J, Carignano MA, Szleifer I. Proc Natl Acad Sci USA 2000; 97:9037.
[5] Klein J, Perahia D, Warburg S. Nature 1991;352:143.
[6] Pincus P. Macromolecules 1991;24:2912.
[7] Ito Y, Ochiai Y, Park YS, Imanishi Y. J Am Chem Soc 1997;119:1619.
[8] Ionov L, Minko S, Stamm M, Gohy JF, Jérôme R, Scholl A. J Am Chem Soc 2003;125:8302.
[9] Wu T, Efimenko K, Genzer J. J Am Chem Soc 2002;124:9394.
[10] Feng JX, Haasch RT, Dyer DJ. Macromolecules 2004;37:9525.
[11] Minko S, Müller M, Motornov M, Nitschke M, Grundke K, Stamm M. J Am Chem Soc 2003;125:3896.
[12] Mansky P, Liu Y, Huang E, Russell TP, Hawker CJ. Science 1997;275: 1458.
[13] Zhao B, Brittain WJ, Zhou WS, Cheng SZD. Macromolecules 2000;33: 8821.
[14] Zhao B, Brittain WJ, Zhou WS, Cheng SZD. J Am Chem Soc 2000;122: 2407.
[15] Zhao B, Haasch RT, MacLaren S. J Am Chem Soc 2004;126:6124.
[16] Lin YH, Teng J, Zubarev ER, Shulha H, Tsukruk VV. Nano Lett 2005;5: 491.
[17] Zhulina EB, Singh C, Balazs AC. Macromolecules 1996;29:6338.
[18] Zhulina EB, Singh C, Balazs AC. Macromolecules 1996;29:8254.
[19] Zhulina EB, Balazs AC. Macromolecules 1996;29:2667.
[20] Minko S, Müller M, Usov D, Scholl A, Froeck C, Stamm M. Phys Rev Lett 2002;88:035502-1.
[21] Wenning L, Müller M, Binder K. Europhys Lett 2005;71:639.
[22] Lotz B, Kovacs AJ. Kolloid Z Z Polym 1966;209:97.
[23] Chen WY, Zheng JX, Cheng SZD, Li CY, Huang P, Zhu L, et al. Phys Rev Lett 2004;93:028301-1.
[24] Zheng JX, Xiong HM, Chen WY, Lee KM, Van Horn RM, Quirk RP, et al. Macromolecules 2006;39:641.
[25] Chen WY, Li CY, Zheng JX, Zhu L, Huang P, Ge Q, et al. Macromolecules 2004;37:5292.
[26] Miyata T, Masuko T. Polymer 1997;38:4003.
[27] De Santis P, Kovacs AJ. Biopolymers 1968;6:299.
[28] Hoogsteen W, Postema AR, Pennings AJ, Ten Brinke G, Zugenmaier P. Macromolecules 1990;23:634.
[29] Kobayashi J, Asahi T, Ichiki M, Okikawa A, Suzuki H, Watanabe T, et al. J Appl Phys 1995;77:2957.
[30] Moskovits M. Rev Mod Phys 1985;57:783.
[31] Otto A, Mrozek I, Grabhorn H, Akemann W. J Phys Condens Matter 1992;4:1143.
[32] Hendra P, Hones C, Warnes G. Fourier transform Raman spectroscopy. New York: Ellis Horwood; 1991. p. 228–59.
[33] Weast RC, editor. Handbook of chemistry and physics. New York: CRC Press; 1980.
[34] Walheim S, Boltau M, Mlynek J, Krausch G, Steiner U. Macromolecules 1997;30:4995.